APPLIED PHYSICS LETTERS **91**, 033508 (2007)

Fabrication and characterization of metal-molecule-silicon devices

Adina Scott and David B. Janes[a]
School of Electrical and Computer Engineering and Birck Nanotechnology Center, Purdue University, Indiana 47907-1285

Chad Risko and Mark A. Ratner
Department of Chemistry, Northwestern University, Illinois 60208

(Received 8 November 2006; accepted 28 May 2007; published online 18 July 2007)

Metal-molecule-silicon (MMSi) devices have been fabricated, electrically characterized, and analyzed. Molecular layers were grafted to *n* and *p*+ silicon by electrochemical reduction of *para*-substituted aryl-diazonium salts and characterized using standard surface analysis techniques; MMSi devices were then fabricated using traditional silicon (Si) processing methods combined with this surface modification. The measured current-voltage characteristics were strongly dependent on both substrate type and molecular head group. The device behavior was analyzed using a qualitative model considering semiconductor depletion effects and molecular dipole moments and frontier orbital energies. © *2007 American Institute of Physics*. [DOI: 10.1063/1.2750516]

Molecular electronic devices to date have been primarily metal-molecule-metal (MMM) devices utilizing thiolated chemistry on gold (Au) substrates.[1] Alternate substrates and attachment chemistries are attractive in terms of bond stability and additional degrees of freedom in device design. Semiconductor (SC) contacts are of particular interest since interactions between the SC bands and molecular levels can lead to interesting effects such as negative differential resistance.[2,3] Due to the dominance of silicon (Si) for electronics applications, metal-molecule-silicon (MMSi) devices are particularly relevant. ⟨111⟩ Si has well-defined surface reconstructions, which allow control of surface structure over large areas. Molecules can be covalently attached to Si using stable Si–O or Si–C bonds.[4] Studies of metal-molecule-semiconductor (MMS) devices have employed degenerate doping and treated the substrate as metal-like[5] or used moderate doping and treated the molecular layer as a small perturbation on a Schottky diode.[6,7] These studies have considered systems in which there are large energy differences between the metal work function (Φ_m), SC Fermi level, and molecular levels. We present a MMS Si device in which the interplay among the metal, molecular levels, and bands of the SC can modulate transport because the valence molecular π orbitals are expected to be near resonance with the contact Fermi energies.

Molecular layers were grafted to ⟨111⟩ *n*-type ($\rho = 0.05-0.1\ \Omega\,\mathrm{cm}$) and *p*+ ($\rho = 0.005-0.001\ \Omega\,\mathrm{cm}$) Si surfaces by hydrogenation and electrochemical grafting of aryl-diazonium salts in aqueous, acidic solution.[8] Si samples were cleaned by repeated sonication in toluene, acetone, and methanol followed by a 15 min immersion in $1:1 H_2SO_4(18M):H_2O_2(30\%)$ and subsequent de-ionized (DI) water rinse. The surface was hydrogen terminated,[9] an InGa eutectic contact was applied and the sample was immediately mounted in the electrochemical cell for molecular grafting.

Aryl-diazonium salts were obtained from Sigma-Aldrich and used without further purification; the as-grafted surface modification species are shown in Fig. 1. Grafting was performed in a three-electrode cell, using the Si (working), a platinum mesh (counter), and a gold wire (pseudoreference). The cell was filled with a dilute solution of sulfuric and hydrofluoric acids in deoxygenated DI water under nitrogen. An appropriate amount of the diazonium salt was dissolved in water and added to the dilute acid in the cell to form a 5 mM molecular solution and an appropriate grafting potential was applied. The current was monitored and the reaction was stopped when approximately monolayer coverage was achieved.[10] The sample was immediately removed from the cell, rinsed with DI water, dried with nitrogen, and ultrasonicated in dichloromethane and acetonitrile.

Molecular layers on unpatterned samples were characterized using x-ray photoemission spectroscopy (XPS) and ellipsometry.[11] XPS confirmed the presence of the molecules on the sample surfaces, and layers showed an oxide thickness equivalent to 12%–18% of an oxide monolayer, except for N-benz, which showed 45% of a monolayer. N 1*s* oxidation energies corresponding to NO as well as NO_2 species were detected in N-benz layers, indicating that some of the head groups were reduced. Ellipsometric measurements yielded relative monolayer thicknesses within ±1 Å of the expected value except for M-benz, which was ≈2 Å larger than expected, indicating partial multilayer formation.

MMSi devices with the structure shown in Fig. 1 were fabricated starting with ⟨111⟩ Si wafers coated with 50 nm of silicon dioxide followed by 200 nm of silicon nitride. Via patterns with 2, 4, 6, and 8 μm diameters were defined using

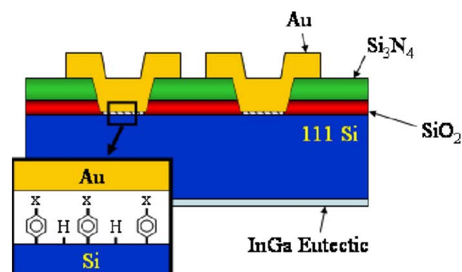

FIG. 1. (Color online) Schematic of MMSi device. The inset shows molecules used in this study, X=Br (B-benz), $N(CH_3)_2$ (D-benz) OCH_3 (M-benz), NO_2 (N-benz).

[a]Electronic mail: janes@ecn.purdue.edu

 © 2007 American Institute of Physics
Downloaded 17 Sep 2009 to 129.105.55.216. Redistribution subject to AIP license or copyright; see http://apl.aip.org/apl/copyright.jsp

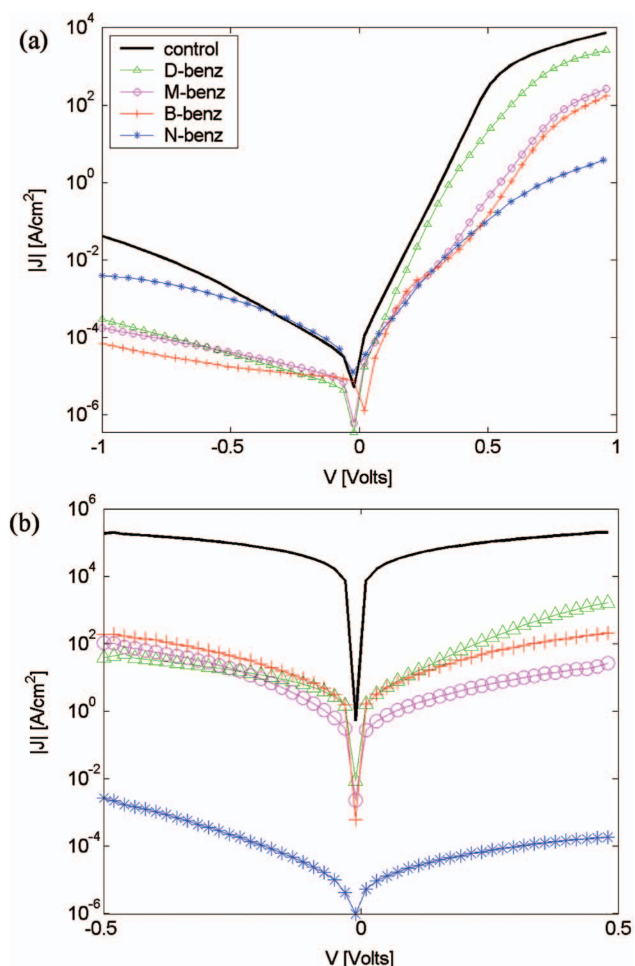

FIG. 2. (Color) Current density vs voltage for MMSi devices on n and $p+$ substrates. The legend graph (a) is applicable to both plots. Note the different measurement ranges for the two plots.

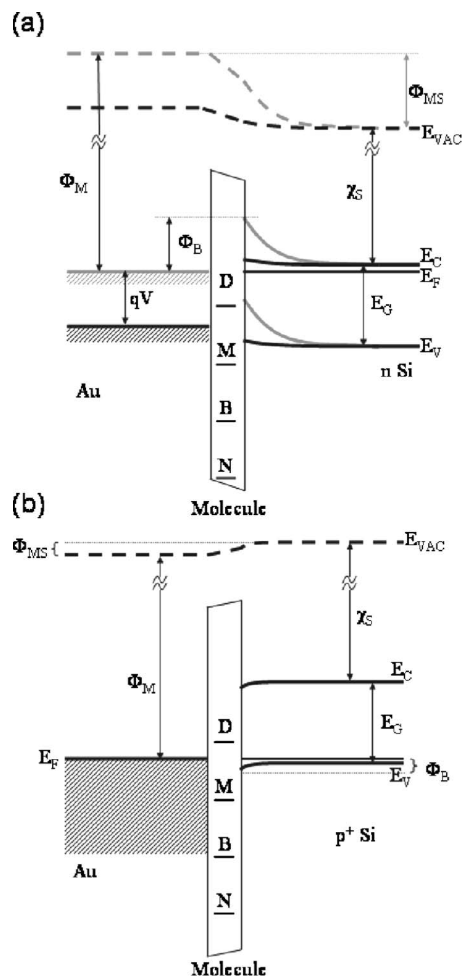

FIG. 3. Proposed energy band diagram for MMSi device with (a) n-Si at equilibrium (gray) and under bias (black) and (b) $p+$ Si. Molecular width is exaggerated for clarity. The horizontal lines in the molecule indicate calculated of HOMO levels with respect to the Au work function under bias.

standard lithography and etching. Following cleaning and molecular grafting, 15–20 nm of Au was deposited using an indirect evaporation process to minimize damage to the molecular layer;[12,13] a 200 nm Au layer was then electron-beam evaporated. Photolithography and etching were used to define contact pads and a large InGa eutectic back contact was applied. Control samples with no molecular layer were introduced into the evaporator within 15 min of the hydrogen-termination etch; Si samples with a native oxide were fabricated by omitting the final etch. The percentage of devices that looked correct upon inspection in an optical microscope ranged from 16% to 100%.

Current-voltage (I-V) measurements were performed at room temperature in the dark with the back contact grounded. For each sample type, at least 40 devices were measured; devices that exhibited I-V curves comparable in shape to those of the majority of the devices and current densities differing by less than 50% from the median value (46–83% of optically ″good″ devices) were considered for further analysis. I-V curves are shown in Figs. 2(a) and 2(b) for MMSi devices on n-Si and $p+$ Si, respectively. Curves are shown for each of the molecular species, obtained by averaging data from at least 40 good devices, as well as the control sample. The I-V characteristics of the oxidized Si samples were indistinguishable from the control samples, indicating that a native oxide does not have significant charge and is not a significant barrier to current flow. Therefore, the partial monolayer of oxide in N-benz is not expected to limit current flow.

MMSi devices can be qualitatively analyzed using approaches from MMM devices,[14] which consider the molecular density of states (DOS) arising from molecular levels which are broadened and shifted by coupling to the contacts. Transport in MMS devices can be described by a compound barrier, comprising (1) a molecular tunnel barrier from the metal through the molecular DOS to the Si surface and (2) a SC barrier from the Si surface through the depletion region to the Si bulk.[15–18] For cases with a depletion region, the SC barrier can be dominant.[16] For appropriate work function offsets or bias conditions, it is also possible to achieve an accumulated Si surface; in this case, the molecule can be the primary barrier. The SC portion of the barrier Φ_B is related to the SC surface potential Φ_S. Band diagrams depicting MMSi devices on n and $p+$ Si are shown in Figs. 3(a) and 3(b), respectively. In an ideal metal-semiconductor (MS) structure, the Φ_B is related to the MS barrier height Φ_{MS}, which arises from the offset between Φ_M and the SC Fermi energy.[18] In a corresponding MMS device, the dielectric nature and dipole moment of the molecule modulate Φ_B. Density functional theory (DFT) calculations of the isolated molecules using the B3LYP functionals[19–21] and a 6-31G** split valence plus double polarization basis set were performed with QCHEM (version 2.0)[22] to assess the molecular electrostatic and elec-

Downloaded 17 Sep 2009 to 129.105.55.216. Redistribution subject to AIP license or copyright; see http://apl.aip.org/apl/copyright.jsp

tronic structure properties . The calculated dipole moments are −2.39, −0.53, 1.96, and 4.56 D for D-benz, M-benz, B-benz, and N-benz, respectively. Φ_S should vary proportionally to the negative of the molecular dipole; however, modulations in Φ_B due to this effect are expected to be small.[23,24] The transparency of the molecular barrier is a function of the molecular DOS in the energy range near the contact potentials, which is related to the molecular electronic levels. Using Koopmans' theorem,[25] the highest occupied molecular orbitals (HOMOs) have calculated ionization (oxidation) energies of 4.76, 5.88, 6.67, and 7.59 eV for D-benz, M-benz, B-benz, and N-benz, respectively. This model predicts that the HOMO energy of D-benz is above the ideal Au Fermi level, whereas those of the other species are below. While these isolated molecular properties can assist with qualitative explanations for the *I-V* curve trends, quantitative statements require consideration of binding to the contacts, which can modulate the molecular dipole moments and orbital energies. More extensive calculation are currently ongoing; recent work has considered long-range cooperative effects and the consequences of model choice for similarly substituted aryl-SAM-Si systems.[26]

For the *n*-type substrates, the control sample is highly rectifying due to the large Φ_{MS}. At negative bias (NB), all samples exhibit low current densities, suggesting that the Si barrier is the dominant current-limiting mechanism. As a positive bias (PB) is applied, the Si bands flatten out as shown in black in Fig. 3(a), leading to a condition where transport through the molecular layer becomes dominant. At 1 V PB, D-benz is the most conductive molecular device, consistent with a HOMO above the Au Fermi energy; in this case, the HOMO would be expected to be partially emptied at low bias, leading to a condition where the molecular level is close to resonance. The trend in conductivities of the other molecular samples is qualitatively consistent with expected transparencies of the molecular barriers, based on the HOMO positions.

For the *p*+ substrates, the control samples exhibit Ohmic behavior consistent with the small Φ_{MS}. The molecular samples are qualitatively different from the control sample, exhibiting asymmetric *I-V* characteristics. Based on the DFT-calculated dipole moments, D-benz devices should be in accumulation and N-benz should have the largest Φ_B, although still much smaller than those on the *n*-type samples, leading to significantly higher conductances. D-benz has higher current density for PB than NB because Φ_B is not a factor due to D-benz being in accumulation; these results point to the application of a PB bringing the higher-lying HOMO closer to resonance with the gold contact. M-benz and N-benz both have higher current densities in NB than PB—consistent with bringing the contact closer to resonance with the HOMO at NB. D-benz and M-benz are much more conductive than N-benz, results consistent with expected trends due to the calculated molecular electrostatic and electronic structure properties. B-benz exhibits fairly symmetric behavior with relatively high current density in both bias directions which would imply a smaller Φ_B and higher HOMO energy than calculated. On both substrate types, M-benz is slightly less conductive than expected relative to B-benz, possibly due to a partial multilayers.

MMSi devices have been fabricated using standard Si processing combined with electrochemical reduction of aryl-diazonium salts. The devices show significant qualitative and quantitative differences for different substrate doping types due to the interplay between the molecular characteristics and the Si bands. When a large Φ_B is present, e.g., for NB in devices on *n* Si, the molecular properties play a modest role. When Φ_B is small as is the case for strong PB in devices on *n* Si and at low bias for devices on *p*+ Si, trends in conductivity correlate with the calculated molecular levels.

The authors would like to thank Dmitri Zemlyanov for XPS. This work is supported by NSF (ECE0506802) and NASA-URETI (NCC3-1363) by the Northwestern MRSEC (DMR-0076097) and NNI-NCN of the NSF and the MURI/DURINT of the DoD. One of the authors (A.S.) is supported by a NSF graduate research fellowship.

[1] A. Salomon, D. Cahen, S. Lindsay, J. Tomfohr, V. B. Engelkes, and C. D. Frisbie, Adv. Mater. (Weinheim, Ger.) **15**, 1881 (2003).
[2] T. Rakshit, G.-C. Liang, A. W. Ghosh, M. C. Hersam, and S. Datta, Phys. Rev. B **72**, 125305 (2005).
[3] N. P. Guisinger, M. E. Greene, R. Basu, A. S. Baluch, and M. C. Hersam, Nano Lett. **4**, 2004 (2004).
[4] J. M. Buriak, Chem. Commun. (Cambridge) **1999**, 1051.
[5] W. Wang, T. Lee, M. Kamdar, M. A. Reed, M. P. Stewart, J.-J. Hwang, and J. M. Tour, Superlattices Microstruct. **33**, 217 (2003).
[6] Y.-L. Loo, D. V. Lang, J. A. Rogers, and J. W. P. Hsu, Nano Lett. **3**, 913 (2003).
[7] Y. Selzer, A. Salomon, and D. Cahen, J. Phys. Chem. B **106**, 10432 (2002).
[8] P. Allongue, C. H. de Villeneuve, J. Pinson, F. Ozanam, J. N. Chazalviel, and X. Wallart, Electrochim. Acta **43**, 2791 (1998).
[9] G. S. Higashi, Y. J. Chabal, G. W. Trucks, and K. Raghavachari, Appl. Phys. Lett. **56**, 656 (1990).
[10] P. Allongue, C. H. de Villeneuve, G. Cherouvrier, R. Cortes, and M.-C. Bernard, J. Electroanal. Chem. **550–551**, 161 (2003).
[11] See EPAPS Document No. E-APPLAB-90-071725 for surface characterization data via a direct link in the online article's HTML reference section or via EPAPS homepage (http://www.aip.org/pubservs/epaps.html).
[12] R. M. Metzger, T. Xu, and I. R. Peterson, J. Phys. Chem. B **105**, 7280 (2001).
[13] S. Lodha and D. B. Janes, J. Appl. Phys. **100**, 024503 (2006).
[14] S. Datta, *Quantum Transport: Atom to Transistor* (Cambridge University Press, New York, 2005), pp. 217–251.
[15] S. Lodha and D. B. Janes, Appl. Phys. Lett. **85**, 2809 (2004).
[16] S. Lodha, P. Carpenter, and D. B. Janes, J. Appl. Phys. **99**, 024510 (2006).
[17] R. L. McCreery, U. Viswanathan, R. P. Kalakodimi, and A. M. Nowak, Faraday Discuss. **131**, 33 (2005).
[18] Simon M. Sze, *Physics of Semiconductor Devices*, 2nd ed. (Wiley-Interscience, New York, 1981), pp. 245–297.
[19] A. D. Becke, Phys. Rev. A **38**, 3098 (1988).
[20] A. D. Becke, J. Chem. Phys. **98**, 5648 (1993).
[21] C. Lee, W. Yang, and R. G. Parr, Phys. Rev. B **37**, 785 (1988).
[22] J. Kong, C. A. White, A. I. Krylov, D. Sherrill, R. D. Adamson, T. R. Furlani, M. S. Lee, A. M. Lee, S. R. Gwaltney, T. R. Adams, C. Ochsenfeld, A. T. B. Gilbert, G. S. Kedziora, V. A. Rassolov, D. R. Maurice, N. Nair, Y. Shao, N. A. Besley, P. E. Maslen, J. P. Dombroski, H. Daschel, W. Zhang, P. P. Korambath, J. Baker, E. F. C. Byrd, T. Van Voorhis, M. Oumi, S. Hirata, C.-P. Hsu, N. Ishikawa, J. Florian, A. Warshel, B. G. Johnson, P. M. W. Gill, M. Head-Gordon, and J. A. Pople, J. Comput. Chem. **21**, 1532 (2000).
[23] P. Hartig, Th. Dittrich, and J. Rappich, J. Electroanal. Chem. **524–525**, 120 (2002).
[24] H. Haick, M. Ambrico, T. Ligonzo, R. T. Tung, and D. Cahen, J. Am. Chem. Soc. **128**, 6854 (2006).
[25] T. Koopman, Physica (Amsterdam) **1**, 104 (1933).
[26] D. Deutsch, A. Natan, Y. Shapira, and L. Kronik, J. Am. Chem. Soc. **129**, 2989 (2007).

Downloaded 17 Sep 2009 to 129.105.55.216. Redistribution subject to AIP license or copyright; see http://apl.aip.org/apl/copyright.jsp